Extended Abstracts of the 2011 International Conference on Solid State Devices and Materials, Nagoya, 2011, pp88-89

# Investigation of Temperature Dependence on DC and Low-Frequency Noise Characteristics in Uniaxial Tensile Strained nMOSFETs

Shih Chang Tsai[1], San Lein Wu[2*], Jone F. Chen[1], Shoou Jinn Chang[1], Ching Yao Chang[1], Po Chin Huang[1], Chung Yi Wu[2], Ming Shing Chen[3], Yao Chin Cheng[3], and Osbert Cheng[3]

[1] Institute of Microelectronics and Department of Electrical Engineering, Advanced Optoelectronic Technology Center, Center for Micro/Nano Science and Technology, National Cheng Kung University, Tainan City 701, Taiwan

[2] Department of Electronic Engineering, Cheng Shiu University, Kaohsiung City 833, Taiwan

[3] Central R&D Division, United Microelectronics Corp. (UMC), Tainan City 744, Taiwan

Phone: +886-7-7310606 ext. 3200 Fax: +886-7-7331758 *e-mail: slwu@csu.edu.tw

## 1. Introduction

The continued shrinking of conventional CMOS devices to achieve enhanced performance has revealed limitations, strain engineering provides the promising method for improving device performance stemming from mobility enhancement [1, 2]. The deposed highly tensile stress SiN film as the contact etch-stop layer (CESL) has attracted much interest because it can provide a significant performance boost for nMOSFETs [3, 4]. On the other hand, the low-frequency (1/*f*) noise is also being a concern for continuously scaling down CMOS devices [5]. This is due to the 1/*f* noise increases as the reciprocal of the device area, which may lead to serious limitation of functionality of the analog, digital, mixed-signal, and RF circuits [6].

In general, Si devices exhibit better performances at low temperatures due to higher carrier mobility [7] and reduced leakage currents [8]. However, with the expansion of electronics into new areas, Si-based electronic devices are now used extensively in many hostile environments, in particular under temperatures exceeding normal operating range. The behaviors of devices operating under high temperature are necessary to be addressed, but relatively little literatures are available for not only DC but also 1/*f* noise characteristics of strained devices. In this paper, we explore the effect of temperature on the DC and 1/*f* characteristics of uniaxial tensile strained nMOSFETs.

## 2. Experiment

The nMOSFETs used in this work were fabricated by the 40-nm technology CMOS process. During the process of CESL, the SiN film with and without tensile stress were deposed on strained and unstrained nMOSFETs, respectively, i.e., CESL and Control devices. All the devices have the same equivalent oxide thicknesses (EOT) of 1.7 nm. All the devices were characterized by an on-wafer test under the temperature ranging from 298 K to 398 K. The 1/*f* noise measurements in a frequency range of 1 Hz to 1k Hz were carried out using the battery-powered SR570 Low-Noise Current Preamplifiers and the Agilent 35670A Dynamic Signal Analyzer.

## 3. Results and Discussion

Fig. 1 shows the drain current ($I_D$) variation with temperature of Control and CESL devices at a fixed gate voltage overdrive, $V_G - V_T = 1$ V, and $V_D = 1$ V using the same gate width to gate length ratio of 1 μm/ 0.044 μm. The enhanced $I_D$ observed from the CESL device indicates higher tensile stress in the channel, proving CESL process-induced stress is truly transmitted from the deposited SiN layer. The $I_D$ degradation of both devices with increased temperature is found due to phono scattering becomes much severer at high temperature, resulting in further decrease in carrier mobility [9]. It can be seen the $I_D$ degradation rate, defined as ($I_D$ @ 398 K - $I_D$ @ 298 K)/ $I_D$ @ 298 K, of 14.62 % for CESL devices is smaller than that of the Control device (17.06 %). The extracted slope of $1.516\times10^{-6}$ A/K for CESL device is also lower than that of Control device ($1.724\times10^{-6}$ A/K). To further explore the characteristics of strained devices operating at high temperatures, the electron mobility is also extracted from the measured maximum extrinsic transconductance at the linear region as illustrated in Fig. 2. It can be seen the mobility degradation ratio of CESL device is less than that of Control counterpart, as the temperature increased from 298 K to 398 K (Fig. 3). These observations indicated that the CESL device is less sensitive to the temperature, and can be ascribed by following the explanations. As compared with the Control device, CESL devices have more tensile stress. This will lead to the larger band splitting between the low-energy Δ2 valleys and high-energy Δ4 valleys, and the preferential occupation of the Δ2 valleys, resulting in an averaged heavier out-of-plane effective mass of electrons [10]. Under the operation of same high temperature, larger band splitting in CESL device induces the reduced intervally phonon scattering and less percentage of electrons having enough thermal energy in Δ2 valleys to emit into Δ4 valleys at the same time. In addition, the increase in out-of-plane electron mass and electron tunneling barrier height bring about the lower tunneling probability [11], resulting in lower gate tunneling current and less gate tunneling current sensitivity to temperature are both observed in CESL device as shown in Fig. 4.

The 1/*f* noise is measured on the large-area devices to avoid the large spreading in results. The normalized drain current noise spectral density ($S_{ID}/I_D^2$) versus the frequency under various temperatures for Control and CESL nMOSFETs are shown in Fig. 5. For both devices, 1/*f* noise shows variation with temperature, and all the slope of the spectrum closes to one. Fig. 6 shows $S_{ID}/I_D^2$ and $(g_m/I_D)^2$ versus $I_D$ for both devices. The $S_{ID}/I_D^2$ curves for both devices exhibits a fairly good proportionally with $(g_m/I_D)^2$ except for strong inversion at all temperature. Also, the extracted Hooge parameters ($\alpha_H$) are between $2\times10^{-3}$ and $2\times10^{-6}$ (Fig. 7), while the associated input-referred voltage spectral noise ($S_{VG} = S_{ID}/g_m^2$) presents a parabolic dependence with gate voltage overdrive ($V_G - V_T$) at strong inversion region (Fig. 8). These results indicate that, regardless of increasing temperature, the physical mechanism of 1/*f* noise for both devices can be described by the correlated number-mobility fluctuation [12]. On the other hands, it can be seen the variation of $S_{ID}/I_D^2$ and $\alpha_H$ with increased temperature in CESL device is rather less than those of Control one. Previous literature have reported that the uniaxial tensile stress improve 1/*f* noise behavior in short channel nMOSFETs [13]. Hence, our experiment results imply the CESL-process-induced tensile stress still slightly transferred to channel even if the gate length is longer, and further exerts its influence as temperature increased. Moreover, the $S_{VG}$ can be express as [5]

$$S_{VG} = \frac{q^2 kT}{WLC_{OX}^2 f}\lambda N_t[1+\alpha\mu_0 C_{OX}(V_G - V_T)]^2 \qquad (1)$$

where λ is the tunneling attenuation length, $N_t$ is the oxide trap density, α is the scattering coefficient, and $\mu_0$ is the carrier mobility. According to the Eq. (1), as shown in Fig. 8, the level of $S_{VG}$ in the region I and the curvature of $S_{VG}$ in the region II can be determined by $\lambda N_t$ and $\alpha\mu_0$, respectively. In region I, for CESL device, the lower $S_{VG}$ level at high temperature indicates the reduced λ because the $N_t$ can be excluded resulting from the comparable amount between both devices under various temperature as shown in Fig. 9. As temperature increased, the slightly smaller curvature of $S_{VG}$ of CESL device in the region II indicates the product of $\alpha\mu_0$ is smaller than that of Control device. It can be ascribed by the stress induced lower carrier scattering and increased mobility at the same time. Consequently, the better 1/*f* noise behavior of strained device at high temperature can be observed, and it can be expected the further pronounced improvement in short channel nMOSFETs with process-induced tensile stress.

### 4. Conclusions

In this paper, we have investigated the temperature dependence of DC and 1/*f* noise characteristics of uniaxial tensile stained nMOSFETs. Base on our experiment results, it is found that the strained device exhibits less sensitivity to temperature, including driving current and gate leakage current. Besides, the improved 1/*f* noise is also observed at higher temperature. These results present the intrinsic benefits of process-induced strained device operating at high temperature.


### Acknowledgements

This work was supported by the National Science Council (NSC) of Taiwan, under Contract No. NSC 99-2221-E-230-019.



### References

[1] C. Hu, *VLSI Symp. Tech.*, p. 4, 2004. [2] S. E. Thompson *et al.*, *IEEE Trans. Electron Devices*, **53**, p. 1010, 2006. [3] F. Ootsuka *et al.*, *IEDM Tech. Dig.*, p. 575, 2000. [4] A. Shimizu *et al.*, *IEDM Tech. Dig.*, p. 19.4.1, 2002. [5] G. Ghibaudo *et al.*, *Microelectron. Reliab.*, **42**, p. 573, 2002. [6] Y. Nemirovsky *at al.*, *IEEE Trans. Electron Devices*, **48**, p. 921, 2001. [7] G. Ghibaudo *et al.*, *J. Phys. IV France*, **06**, p. 3, 1996. [8] V. Gaspari *et al.*, *Appl. Surf. Sci.*, **224**, p. 390, 2004. [9] K. Chainy *et al.*, *Semicond. Sci. Technol.*, **12**, p. 355, 1997. [10] S. I. Takagi *et al.*, *IEDM. Tech. Dig.*, p. 219, 1997. [11] Wei Zhao *et al.*, *IEEE EDL.*, **26**, p. 410, 2005. [12] K. K. Hung *et al.*, *IEEE Trans. Electron Devices*, **37**, p. 654, 1990. [13] C. W. Kuo *et al.*, *APL*, **97**, p. 123501, 2010.


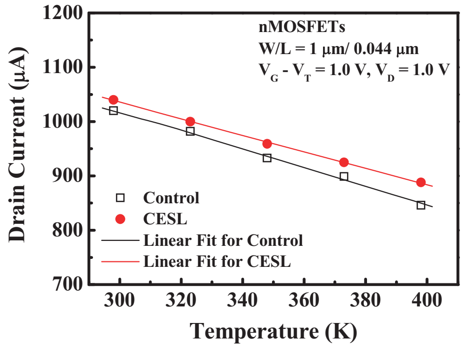


Fig. 1 Drain current variation with temperature at a fixed gate overdrive, $V_G$ - $V_T$ = 1 V, and $V_D$ = 1 V for Control and CESL nMOSFETs.

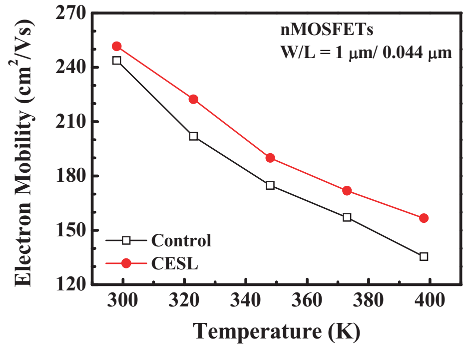


Fig. 2 Electron mobility variation with temperature for Control and CESL nMOSFETs.

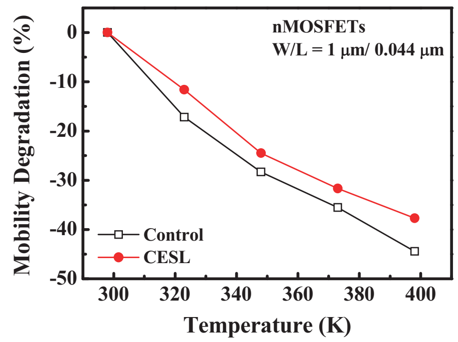


Fig. 3 The temperature dependence of the mobility degradation, defined as (μ @ T K - μ @ 298 K)/ μ @ 298 K.

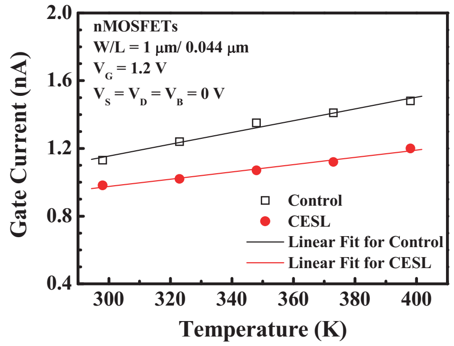


Fig. 4 Gate current variation with temperature at a fixed gate voltage ($V_G$ = 1.2 V) for Control and CESL nMOSFETs.

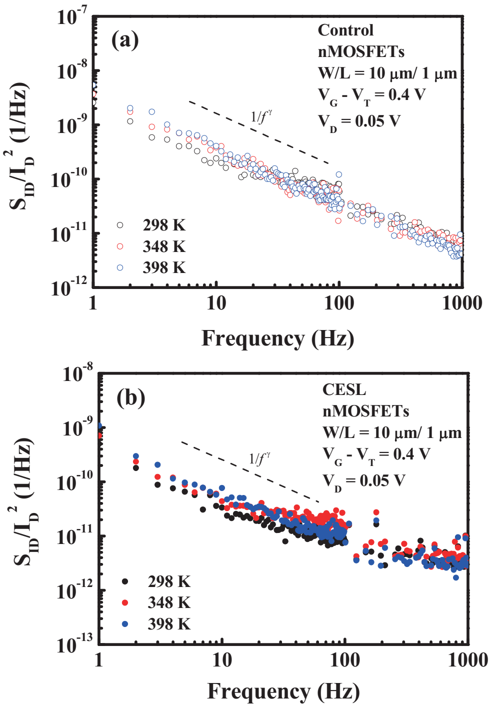


Fig. 5 Normalized drain current noise spectral density ($S_{ID}/I_D^2$) versus the frequency for (a) Control and (b) CESL nMOSFETs under various temperature.

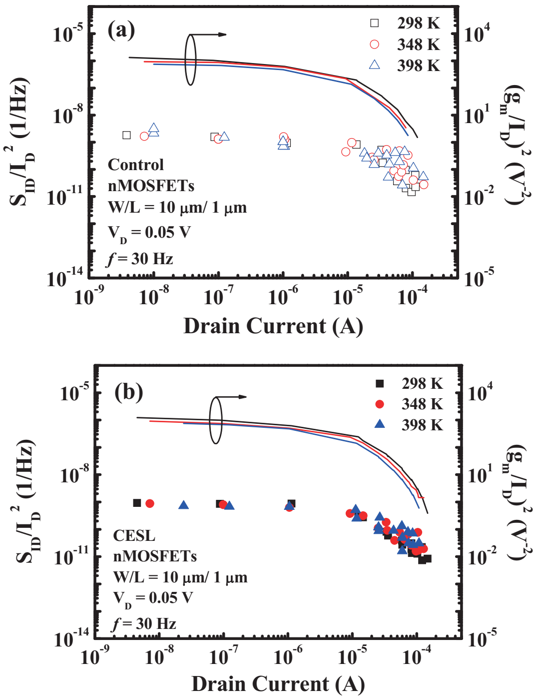


Fig. 6 Normalized drain current noise spectral density ($S_{ID}/I_D^2$) and transconductance-to-drain-current ratio squared $(g_m/I_D)^2$ versus drain current for (a) Control and (b) CESL nMOSFETs under various temperature.

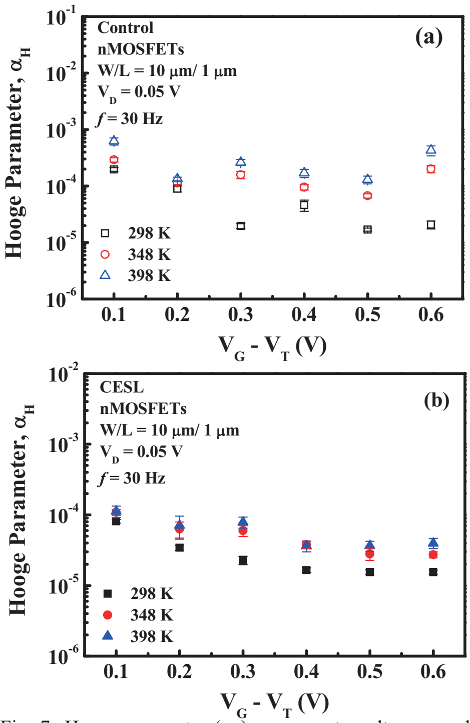


Fig. 7 Hooge parameter ($\alpha_H$) versus gate voltage overdrive ($V_G$ - $V_T$) for (a) Control and (b) CESL nMOSFETs under various temperature.

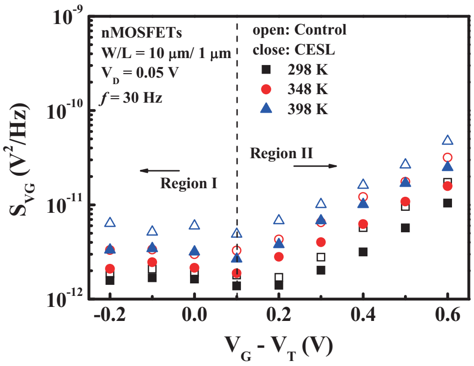


Fig. 8 Normalized input-referred voltage noise ($S_{VG}$) versus gate voltage overdrive ($V_G$ - $V_T$) for Control and CESL nMOSFETs under various temperature.

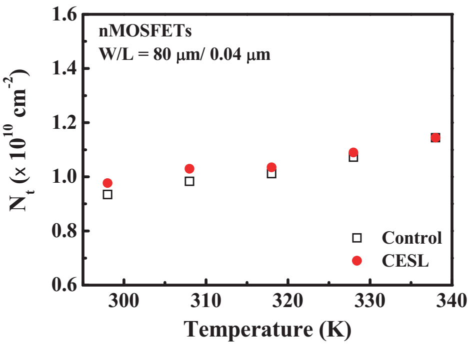


Fig. 9 Interface trap ($N_t$) variation with temperature for Control and CESL nMOSFETs, extracted from charge pumping measurement.